PERINATAL JOURNAL

Original Article

Perinatal Journal 2026; 34(1):227-238

https://doi.org/10.57239/prn.26.03410026

The effect of nano ZNO and nano iron oxide on the expression of some genes of pathogenic escherichia coli bacteria

Halah Kamal Al-Qazzaz[a*], Muntaha R. Ibraheem[b]

[a]Department of Biotechnology, College of Science, University of Baghdad, Iraq
[b]Department of Biomedical Engineering, Al-Khwarizmi College of Engineering, University of Baghdad, Baghdad, Iraq

Abstract

Escherichia coli is a major contributor to biofilm-associated Urinary Tract Infections (UTIs) and has shown increasing resistance to conventional therapies. Nanotechnology offers a promising alternative approach to overcome this challenge. This study aimed to evaluate the anti-biofilm activity of zinc oxide and iron oxide nanoparticles against E. coli and to investigate the regulatory role of the csgD gene in biofilm formation. A total of 50 E. coli isolates were obtained, including 25 from UTI patients (case group) and 25 from healthy individuals (control group). The isolates were cultured, and biofilm formation was evaluated using the microtiter plate test, measuring op-tical density at 600 nm (OD_{600}). The results of gene expression showed upregulation of the csgD gene, associated with the inhibition of biofilm formation by UPEC using ZnO and Fe_2O_3 nanopar-ticles. These results indicate that the effect of NPs on biofilm formation uses a biomarker to in-hibit the growth of UPEC.

Keywords: Curlin subunit gene D, Invasion of epithelial cells, ZnO, Fe_2O_3, UPEC

1.Introduction

Escherichia coli is the pathogen isolated from Urinary Tract Infections (UTIs), with Ur pathogenic *Escherichia coli* (UPEC) accounting for the majority of infections in females and children [1]. The pathogenesis of UPEC is characterized by the production and formation of biofilms, a structured microbial population enclosed inside a self-produced extracellular polymeric substance (EPS) matrix that exhibits increased tolerance to antimicrobial treatment, complicating infections [2]. In addition, expressing adhesive factors such as type 1, P, S, and F1C pili, UPEC causes UTI by adherence to urinary tract epithelial cells and allows the bacterium to display characteristics like motility, biofilm formation, and antibiotic resistance [3,4]. Biofilm is a community of bacteria that embeds in an exopolysaccharide matrix. Bacteria within the biofilm are protected from environmental stresses such as dryness, host immune responses, and antimicrobial substances, which promote Multidrug Resistance (MDR) and chronic infection [5,6]. Different surface structures, such as type 1 fimbriae, curli, PGA polysaccharides, clavulanic acid, flagella, and antigen 43 (Ag43), are involved in the biofilm formation process [7]. Patients with urinary catheters have a higher risk of acquiring UTIs, and biofilm formation on the catheter after seven days of catheterization leads to UTI [8]. Treatment of UTI imposes a substantial economic burden on the healthcare systems around the world. Biofilm development in *E. coli* comprises multiple stages: the initial adhesion, second, quorum Sensing (QS), and final microcolony formation and maturation. Structures such as type I fimbriae and curli fibers play a central role in adhering and forming biofilm. *Escherichia coli* is the major pathogen isolated from UTIs, with UPEC accounting for the majority of infections in females and children [9]. The pathogenesis of UPEC is characterized by the production and formation of biofilms, a structured microbial population enclosed inside a self-produced Extracellular Polymeric Substance (EPS) matrix that exhibits increased tolerance to antimicrobial treatment, complicating infections [10]. In addition to expressing adhesive factors, such as type 1, P, S, and F1C pili, UPEC causes adherence to urinary tract epithelial cells, allowing the bacterium to display characteristics like motility, biofilm formation, and antibiotic resistance [11]. Biofilm is a community of bacteria that embeds in an exopolysaccharide matrix. Patients with urinary catheters have a higher risk of acquiring UTIs, and

Correspondence: Halah Kamal Al-Qazzaz, Department of Biotechnology, College of Science, University of Baghdad, Iraq., **e-mail:** halah.k@sc.uobaghdad.edu.iq, **Received:** October 16, 2025 **Accepted:** December 6, 2025

biofilm formation on the catheter after seven days of catheterization leads to UTIs [12]. Biofilm development in *E. coli* comprises multiple stages: the initial adhesion, second, Quorum Sensing (QS), and final microcolony formation and maturation. Structures such as type I fimbriae and curli fibers play a central role in adhering to and biofilm formation [13]. The QS system production of autoinducers (e.g., AI-2 via the luxS gene) coordinates gene expression based on bacterial population density [14]. Inhibition of biofilm formation can be achieved by targeting QS pathways, adhesion mechanisms, or disrupting the EPS matrix [15,16]. Several genes were identified as central to *E. coli* biofilm regulation. The *fimH* gene encodes fimbria adhesins essential for attachment, while *bolA* is associated with the production of curli and fimbriae [17,18]. The Curlin Subunit Gene D (*csgD*) plays a pivotal role as a transcriptional regulator of curli biosynthesis and cellulose production, as well as attractive surface adhesion and biofilm maturation [19]. Nanoparticles (NPs), particularly metal-based NPs such as Zinc Oxide (ZnO) and iron oxide (Fe_2O_3), exhibit broad-spectrum antibacterial properties that interfere with bacterial membranes, generate reactive oxygen species (ROS), and disrupt vital cellular processes [20]. Biofilm formation, antibiotic resistance, and nanotechnology have emerged as promising approaches in antimicrobial therapy. The ZnO NPs, in particular, are considered safe for human use and have been applied in drug delivery, bioimaging, and antimicrobial formulations [21]. Nevertheless, their ability to disrupt biofilms and inhibit gene expression is associated with virulence factors. This study aims to investigate the anti-biofilm activity of ZnO and Fe_2O_3 NPs against UPEC isolates from UTI patients and to elucidate the role of the *csgD* gene in biofilm regulation and stress response. The QS system production of autoinducers (e.g., AI-2 via the luxS gene) coordinates gene expression based on bacterial population density [22]. Inhibition of biofilm formation can be achieved by targeting QS pathways, adhesion mechanisms, or disrupting the EPS matrix. Several genes were identified as central to *E. coli* biofilm regulation. The fimH gene encodes fimbria adhesins essential for attachment, while bolA is associated with the production of curli and fimbriae [23]. The *csgD* gene plays a pivotal role as a transcriptional regulator of curli biosynthesis and cellulose production, as well as attractive surface adhesion and biofilm maturation. Nanoparticles (NPs), particularly metal-based NPs such as Zinc Oxide (ZnO) and iron oxide (Fe_2O_3), exhibit broad-spectrum antibacterial properties that interfere with bacterial membranes, generate Reactive Oxygen Species (ROS), and disrupt vital cellular processes [24]. Biofilm formation, antibiotic resistance, and nanotechnology have emerged as promising approaches in antimicrobial therapy. The ZnO NPs, in particular, are considered safe for human use and have been applied in drug delivery, bioimaging, and antimicrobial formulations [25]. Nevertheless, their ability to disrupt biofilms and inhibit gene expression is associated with virulence factors. This study aims to investigate the anti-biofilm activity of ZnO and Fe_2O_3 NPs against UPEC isolates from UTI patients and to elucidate the role of the *csgD* gene in biofilm regulation and stress response.

2. Research Methodology

2.1 Sampling

The study design was a case-control prospective study involving 50 Iraqi individuals of different ages, including 25 bacterial isolate samples from UTI patients as cases and 25 healthy individuals as controls, collected from inpatients and outpatients at Baghdad Hospital between January and March 2025. Urine samples of approximately 5-10 ml were collected in a sterile cap from individuals in study groups and were immediately sent to the laboratory for traditional examination within 2 h. This study was approved by the Council of the College of Science/University of Baghdad and Al-Yarmouk Hospital. All experimental study work was conducted in accordance with the declaration of the Human Ethics Committee of the Ministry of Health in Iraq.

2.1.1 Microbial culture

One microliter of urine was cultured onto a MacConkey agar plate and incubated at 37°C for 24 to 48 h to detect *E. coli*. Gram staining was employed to identify the colonies based on their morphology. Three microliters of the bacterial suspension were used for biochemical identification by the VITEK-2 system, following the manufacturer's instructions (bioMérieux, France). The isolated *E. coli* was tested for antibiotic susceptibility using the VITEK 2 AST-N222 Method to *investigate* biofilm formation. Molecular studies were conducted to detect and

express virulence factor genes for *E. coli* biofilm formation.

2.2 Biofilm inhibition assay

Mueller-Hinton broth (MHB), 199 µL, was placed in a microplate and supplemented with 1% glucose. The microplate was inoculated with 20 µL from suspended isolates of about 0.5 to 0.7 McFarland (1.10^8 cfu/mL) and incubated for 24 h at 37°C without agitation. It was washed twice with phosphate-buffered saline (PBS). The crystal violet was used to observe bacterial adherence in a 96-well plate. The microplate dye of biofilms in the walls of the microplate is resolubilized by 150 µL of 95% ethanol. After 5-10 min, the microplate is measured for the optical density (OD) at 560 nm by a microplate reader. The GloMax® Discover Microplate Reader was used to measure the OD value of biofilm formation (Promega, USA) and classify the strains as follows: strong ≥0.3, moderate ≥0.2, and weak ≥0.1. The MIC was determined by determining the lowest concentration of NPs that completely inhibited the growth of the isolates [26;27].

2.2.1 Preparation of ZnO and Fe_2O_3 Nanoparticles

The minimum inhibitory concentration (MIC) was determined for biofilm formation using different concentrations of ZnO and Fe_2O_3 NPs with a microtiter plate method. The NPs were prepared to an approximate size of 10 to 30 nm by mixing the powder with propylene glycol at various concentrations (0.1-5 mg/mL) and sterlized at 160°C for 3 hours using A 4 mg/mL bacterial suspension as a stock solution for susceptibility evaluation [28].

2.3 Molecular study

Genomic DNA extraction

Total DNA was extracted from five isolated strains using Genomic Mini isolation kits (Promega, USA). The concentration and purity of the extracted DNA were determined using a Nanodrop 1000 (Thermo Fisher Scientific).

2.3.1 Genomic detection of E. coli

After dissolving the lyophilized primers in 300 µl of nuclease-free water to produce a stock solution, 10 pmol/µl of primer stock solution is mixed with 90 µl of nuclease-free water to create a working primer solution, which has a final concentration of 100 pmol/µl. The polymerase chain reaction (PCR) mixture included 10 µl of GoTaq® Green Master Mix, 1 µl of forward primer (F), 1 µl of reverse primer (R), 2 µl of ng/µl DNA template, and 6 µl of nuclease-free water to complete the amplification mixture to 20 µl, then placed into the thermocycler PCR machine for 30 cycles. A Veriti thermal cycler was used for amplification, programmed as follows: initial denaturation at 95°C for 5 min, denaturation at 95°C for 30 sec, annealing at 55°C and 60°C for 30 sec, extension at 72°C for 30 sec, and final extension at 72°C for 7 min. The program was held at 4°C for 10 min, and 1.5% gel electrophoresis was used for observation of the PCR products.

Table 1: Oligonucleotide primer sequences for detecting csgD and invE genes in E. coli

Gene	Primer Sequence (5`-3`)	Length of amplified (bp)	Annealing Temp. (˚C)	Reference
csgD-F	TGGACGATATCTCTTCAGGCTC	150	60	macrogen
csgD-R	CGCGGTACGGGTAATCTTCAG			
invE-F	GCAGGAGCAGATCTTGAAG	208	55	
invE-R	GAAAGGCACGAGTGACTTTC			

2.3.1 Expression of csgD and E. co-16s Genes

The RNA was isolated from the samples according to the protocol of the TRIzol™ reagent for molecular studies. The total RNA was extracted using a RNeasy minikit (QIAGEN) according to the manufacturer's instructions, and the RNA samples were converted to cDNA using the SYBR Green master mix in a one-step RT-PCR.

2.3.2 Gene expression of the csgD Gene by RT-PCR

A One Step RT-PCR kit was employed for the *csgD* gene and *E. co-16s* as a housekeeping gene (HKG) (internal reference) that was used for normalization to calculate the target genes according to the Livak

and Schmittgen method (2008). The RT-PCR reaction volume was 10 µl for 40 cycles, including 5 µl of qPCR Master Mix (Promega, USA), 0.25 µl of RT mix, 0.25 µl of $MgCl_2$, 0.5 µl of primers (forward and reverse), 1 µl of ng/µl cDNA, and 2 µl of nuclease-free water to complete the volume to 10 µl using a thermocycler PCR machine. The RT-PCR program

3. Results and Discussion

3.1 Isolation and identification of uropathogenic escherichia coli

Following cultivation on MacConkey agar, *E. coli* isolates were obtained from urine samples. A total of 15 isolates demonstrated typical growth characteristics of UPEC strains. Colonies appeared large, round, and pink due to lactose fermentation, consistent with the selective and differential properties of MacConkey agar. Microscopic examination confirmed the isolates as gram-negative, short, rod-shaped bacilli. The identity of the isolates was further verified through biochemical analysis using the AST VITEK 2 automated system, which provides rapid and accurate species-level identification and antibiotic susceptibility testing [29].

3.2 Antibiotic resistance and antibiofilm assessment using nanoparticles

Antibiotic susceptibility testing was performed on 50 *E. coli* isolates using the agar diffusion method with ZnO and Fe_2O_3 NPs producing 2 to 5 cm in diameter inhibition zones, signifying antimicrobial activity as shown in Fig. 1. The present results confirm that UPEC in urine samples is the predominant causative agent of UTIs. In addition to ZnO NPs, a significantly larger inhibition zone was observed compared to Fe_2O_3 NPs, resulting in greater efficacy in disrupting biofilm and inhibiting bacterial growth. The increased activity can be created by various mechanisms, including the production of ROS, release of Zn^{2+} ions, and rupture of bacterial cell membranes, resulting in oxidative stress and bacterial mortality and lower surface reactivity [30;31]. The results demonstrated and promoted the potential of ZnO NPs as effective antimicrobial and antibiofilm agents against UPEC strains. Such NPs may provide promising alternatives to traditional antibiotics, especially in the context of increasing antimicrobial resistance.

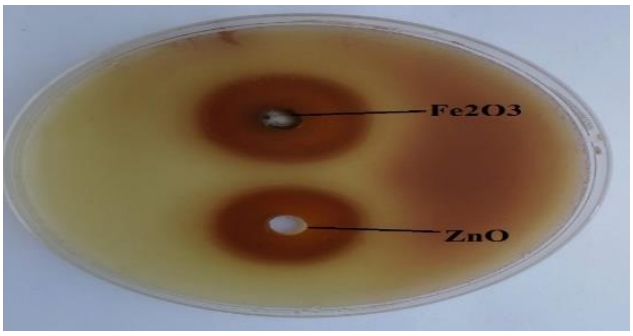

Fig. 1. Biofilm formation using agar diffusion method by ZnO and Fe NPs

3.3 Evaluation of biofilm formation using crystal violet assay

The biofilm production of 12 UPEC isolates was quantitatively assessed using the standard crystal violet microtiter plate assay using an ELISA reader, as shown in Fig. 2. The results revealed different biofilm-forming among the examined isolates. Wells treated with metal oxide NPs, specifically ZnO, showed significantly lower staining intensity compared to untreated controls. The decrease in crystal violet absorption correlates with biofilm biomass, indicating the inhibitory effects of NPs on biofilm development. In contrast, the negative control wells (NC), containing solely sterile broth without bacterial inoculum, displayed no staining, confirming the assay's specificity and reliability. The observed biofilm inhibition supports the idea that metal oxide NPs can markedly disrupt the structural integrity and formation of *E. coli* biofilms [32;33]. The ZnO NPs show significant antibiofilm efficacy properties, likely due to their capacity to produce ROS, release Zn^{2+} ions, and disrupt bacterial membranes. These mechanisms induce cellular stress, compromise membranes, and lead to biofilm formation. Importantly, the successful and effective disruption of biofilms by ZnO NPs could have promising applications in biomedical device coatings, wound dressings, and food packaging, where biofilm formation poses significant hygiene concerns. Surfaces can reduce bacterial adherence and colonization in clinical and industrial environments [34].

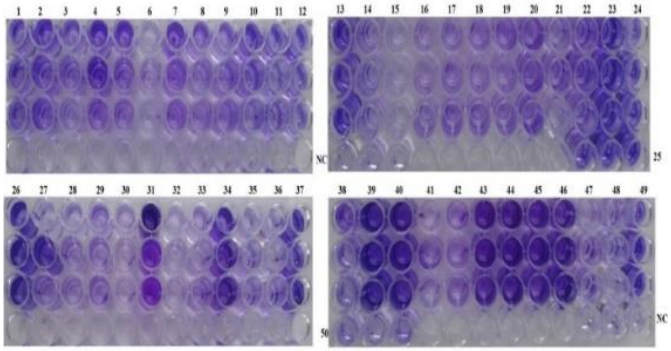

Fig. 2. Evolution of biofilm formation in UPEC using the microtiter plate method. NC: negative control

3.4 Quantitative evaluation of inhibition of biofilm formation for *E. coli*

The quantitative measurement of biofilm formation by *E. coli* isolates was performed using the microtiter plate test, with OD readings obtained via ELISA at 570 nm. As illustrated in Fig. 3, the OD values varied among isolates, indicating different levels of biofilm formation.

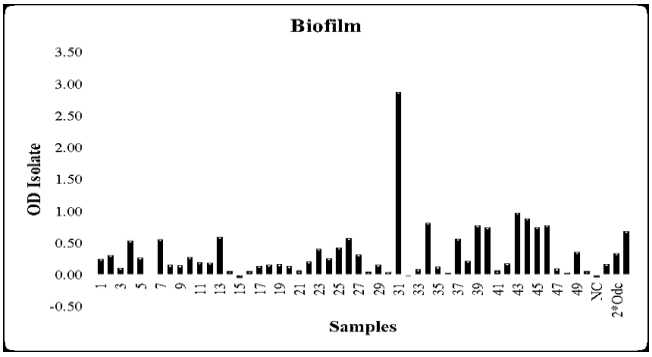

Fig. 3. Quantitative assessment of E. coli biofilm formation inhibition

Isolates with OD values ranging from 2.5 to 3.0 were classified as strong biofilm producers, while those with OD values between 1.5 and 2.0 were considered moderate biofilm formers. A further decline in OD values below 1.5 indicated weak or non-biofilm-producing strains, with readings approaching 0 signifying complete inhibition or absence of biofilm formation. These results reflect the inherent variability in biofilm-forming capacity among clinical *E. coli* isolates and illustrate the potential impact of external interventions such as nanoparticle treatments on suppressing biofilm development. The significance of biofilm formation in clinical settings cannot be overstated. It is estimated that approximately 80% of chronic and recurrent bacterial infections in humans are biofilm-associated, primarily due to the enhanced resistance biofilms confer against antibiotics and host immune responses [35]. Biofilm-associated infections often occur on abiotic surfaces, particularly medical implants, catheters, and other indwelling devices, where *E. coli* can adhere and establish persistent infections. The result of this study corroborates the increasing evidence indicating that disrupting biofilm formation may be a key strategy in reducing device-related and hospital-acquired infections. Recent therapeutic approaches have focused on the use of antibiofilm agents that target various stages of biofilm development, such as initial bacterial adhesion, QS pathways, and synthesis of Extracellular Polymeric Substances (EPS) [36]. The efficacy of these therapies, particularly the use of metal oxide NPs, represents a promising frontier in the management of multidrug-resistant biofilm-forming bacteria like *E. coli*.

3.5 Molecular detection of *CsgD* and *invE* genes

The result of the *E. coli* genetic basis of biofilm formation and PCR amplification performed by two biofilm-related genes: *csgD* and *invE*. Genomic DNA was extracted from 15 clinical *E. coli* isolates, and gene-specific primers were employed to amplify the target sequences. The PCR products were separated by electrophoresis on a 1.5% agarose gel, stained with ethidium bromide, and visualized under a UV transilluminator using a 100 bp DNA ladder as a molecular size marker. Fig. 4 and Fig. 5 illustrate this process.

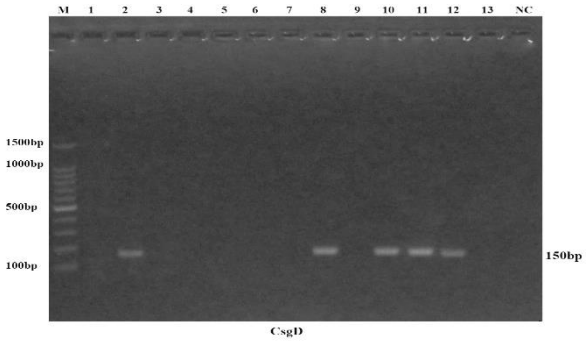

Fig. 4. The amplification of E. coli samples for the CsgD gene was electrophoresed in a 1.5% agarose gel at 5 volts/cm and stained with EtBr. M: Ladder marker 1500 kb; Lanes 1–13 with 105 bp PCR products, and NC: negative control

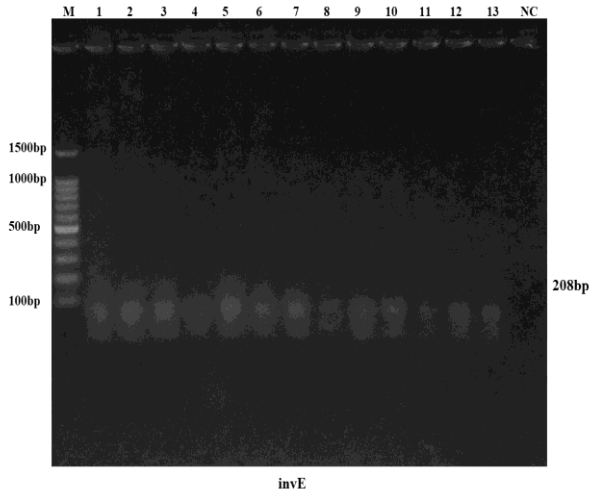

Fig. 5. The amplification of E. coli samples for the CsgD gene was electrophoresed in a 1.5% agarose gel at 5 volts/cm and stained with EtBr. M: Ladder marker 1500 kb; Lanes 1–13 with 208 bp PCR products; and NC: negative control.

The effective identification of the *csgD* gene in these isolates supports its critical role in biofilm formation. The *CsgD* is a master regulator gene that is responsible for the expression of curli fimbriae and cellulose, critical constituents of the biofilm extracellular matrix [37]. The presence of *csgD* in most isolates indicates their strong genetic capacity for biofilm production, correlating well with the phenotypic biofilm formation observed in crystal violet and nanoparticle inhibition assays. The *invE* gene was initially identified and associated with type III secretion systems in enteroinvasive *E. coli* (EIEC) and Shigella spp., the virulence in biofilm development, including adhesion and invasion processes, and host contact [35]. Moreover, it enhances virulence and host tissue colonization. The confirmation of biofilm-associated genes further supports the potential application of metal oxide NPs as anti-biofilm agents targeting genetically biofilm-capable strains of *E. coli*. These molecular discoveries complement the phenotypic data, especially the distinct biofilm inhibition observed with ZnO and Fe_2O_3 NPs.

3.6 Biofilm production and gene expression

The results of the total RNA extraction data for all 15 samples were produced. Biofilm investigation yielded a main concentration with a mean of 406.8 ng/µl, as shown in Table 2.

Table 2: RNA concentration (ng/µl)

Sample	Concentration
C2	393
C8	537
C10	302
C11	381
C12	336
ZN2	477
ZN8	631
ZN10	220
ZN11	409
ZN12	450
Fe_2O_3, 2	232
Fe_2O_3, 8	565
Fe_2O_3, 10	449
Fe_2O_3, 11	292
Fe_2O_3, 12	428
Average	406.8

The total RNA from 15 samples produced biofilm in the study for ZnO and Fe_2O_3 NPs was completely converted to cDNA using one-step RT-PCR, and gave a good product.

3.7 The Effect of ZnO and Fe_2O_3 NPs on the *csgD* gene expression

Quantitative reverse transcription PCR (RT-qPCR) was performed to assess the expression levels of the *csgD* gene in an *E. coli* isolate treated with ZnO and Fe_2O_3 NPs. The 16S rRNA gene was used as an internal control for normalization due to its high conservation and stability in bacterial gene expression studies.

The amplification plot (Fig. 6) showed clear sigmoidal amplification curves for the 16S rRNA gene, indicating efficient and successful reverse transcription and PCR amplification. The cycle threshold (Ct) values ranged from 18 to 28, with a mean Ct of 20.30, representing consistent and reproducible detection across the samples.

The sigmoidal shape of the amplification curves is characteristic of successful real-time PCR, reflecting exponential accumulation of PCR products. The relatively early Ct values (average ~20) confirm the presence of sufficient template cDNA and efficient amplification, particularly for the 16S rRNA gene,which serves as a reliable reference gene in bacterial gene expression analysis [12].

The reliable amplification of the 16S rRNA gene validates the RNA quality and confirms the efficiency of the reverse transcription process. This is crucial for downstream comparison of *csgD* gene expression levels between treated versus untreated *E. coli* groups. Subsequent relative quantification (not shown here but expected in full analysis) would typically be done using the ΔΔCt method to assess changes in *csgD* expression following treatment with ZnO and Fe_2O_3 NPs. If ZnO NPs result in increased Ct values for *csgD* compared to controls (indicating lower expression), this would support the hypothesis that ZnO effectively suppresses biofilm formation at the transcriptional level, consistent with its phenotypic antibiofilm effects. These molecular findings are important because *csgD* functions as the central regulator of biofilm matrix production in *E. coli*, including curli fimbriae and cellulose synthesis [37]. Downregulation of *csgD* following nanoparticle treatment may explain the observed reductions in biofilm biomass, as shown in earlier phenotypic assays.

3.8 Melt curve analysis

The RT-qPCR assay targeting *E. co-16s* rRNA demonstrates high specificity, efficiency, and reproducibility. A sigmoidal amplification curve with appropriate Ct values and single, sharp melt curve peaks strongly indicates successful detection and quantification of the target gene. This result pertains to gene expression studies, microbial quantification, or diagnostic workflows involving *E. coli*.

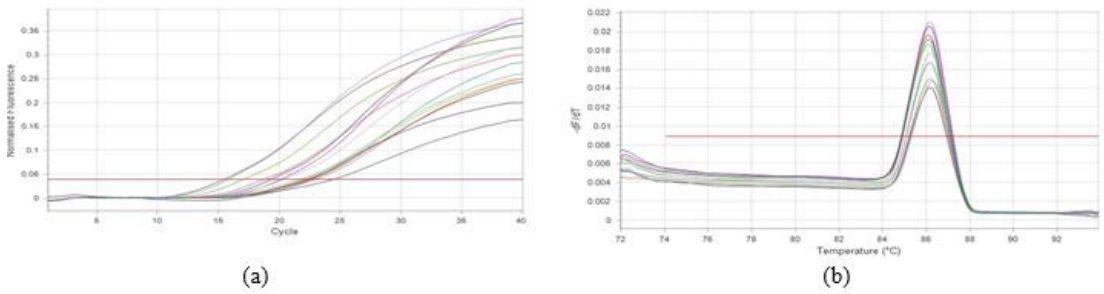

Fig. 6. Melt curve and amplification plots of E co-16s gene amplicons after RT-qPCR

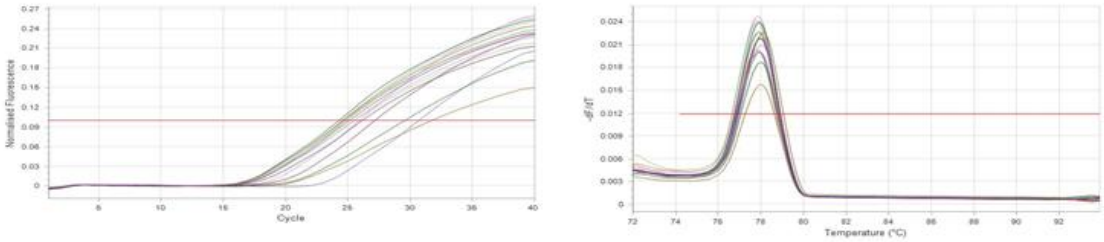

Fig. 7. Melt curve and amplification plots of csgD gene amplicons after RT-qPCR

These results validate the RT-qPCR assays used for both *Eco-16s* rRNA and *csgD* gene targets, supporting their suitability for gene expression analysis. The assay's high specificity and reproducibility ensure accurate quantification, which is essential for assessing the impact of ZnO and Fe_2O_3 NPs on biofilm-regulating gene expression in *E. coli*.

3.9 Biofilm production and gene expression

The result of the expression analysis for biofilm production using the *csgD* gene is presented in Table 3. The mean Ct-value for HKG *E. co-16s* for all samples in the study group was 20.30, which was used as an internal control for normalizing the *csgD* gene expression. On the other hand, the *E. coli*-16s gene Ct-value results for control (2, 8, 10, 11, 12) were 20.11. The result of *csgD* mean Ct-value was 26.37, the mean of ΔCt was 6.26, the ΔΔCt mean was 0, and the fold change ($2^{-\Delta\Delta Ct}$) was 1. This result indicates no regulation for *E. co-16s* for *E. coli* samples (2, 8, 10, 11, 12). On the other hand, the mean Ct-values for *E. co-16s* for ZnO samples (2, 8, 10, 11, and 12) produced

were 19.92. On the other hand, the mean Ct-value for the *csgD* gene was 26.50, the mean of ΔCt was 6.58, ΔΔCt was 0.33, and the fold change was 3.56. This result produces the significant up-regulation of *csgD* for ZnO samples (2, 8, 10, 11, and 12). Moreover, the mean Ct-value for *E. coli*-16s was 20.88 for Fe_2O_3 (2, 8, 10, 11, 12) samples, resulting in a mean Ct-value for the *csgD* gene of 26.2, a mean ΔCt of 5.31, a mean ΔΔCt of -0.95, and a fold change of 5.80. This result produces the significant up-regulation of *csgD* for Fe_2O_3 (2, 8, 10, 11, 12) samples.

Table 3: Gene expression calculation levels for the csgD gene

Groups	Samples	*E.co16s*	*csgD* Ct	ΔCt	ΔΔCt	Fold change
Control	2	22.47	31.76	9.29	0	1
	8	17.01	24.69	7.68	0	1
	10	22.95	24.9	1.95	0	1
	11	22.66	25.92	3.26	0	1
	12	15.44	24.58	9.14	0	1
mean		20.11	26.37	6.26	0	1
ZnO	2	19.49	30.71	11.21	1.93	0.26
	8	15.82	24.73	8.92	1.24	0.42
	10	20.1	25.59	5.49	3.55	0.09
	11	22.25	24.3	2.04	-1.21	2.32
	12	21.92	27.18	5.26	-3.88	14.73
mean		19.92	26.50	6.58	0.33	3.56
Fe_2O_3	2	24.43	29.59	5.16	-4.13	17.5
	8	18.72	26.17	7.44	-0.23	1.18
	10	21.66	24.62	2.96	1.01	0.5
	11	20.34	25.47	5.13	1.88	0.27
	12	19.27	25.15	5.88	-3.26	9.56
mean		20.88	26.2	5.31	-0.95	5.80

$2^{-\Delta\Delta Ct}$: fold change, C2,8,10,11,12: Control *E. coli* ZnO, 2,8,10,11,12 Sample for ZnO strains 1 & 2, S: sample

The expression data for the *csgD* gene were collected under different treatment conditions (control, ZnO, Fe_2O_3) and normalized to the *E. coli* rRNA (HKG). The *csgD* gene encodes a transcriptional regulator in *E. coli* and other Enterobacteriaceae that controls curli fiber production and biofilm formation, playing a critical role in surface adhesion, extracellular matrix production, and survival under stress. The control group shows a relatively stable and later point of departure fold change, which acts as the reference generate ROS and can stress bacterial cells, leading to biofilm-associated gene upregulation as a survival mechanism. The overexpression of ZnO-induced *csgD* may suggest a protective biofilm response to limit Zn^{2+} penetration and ROS damage [38].

The expression pattern suggests a moderate induction of biofilm-associated genes below iron oxide stress. Iron oxides can interact with bacterial membranes and iron metabolism, triggering stress and biofilm gene activation. Iron availability also modulates biofilm dynamics in *E. coli*. Fe_2O_3 may lead to moderate stress, promoting *csgD-mediated* biofilm development, potentially aiding iron sequestration or condition. This reflects normal expression of *csgD* in *E. coli*, which supports biofilm development under standard conditions. In contrast, the high variability of ZnO NPs exerts a heterogeneous impact on *csgD* expression across samples and overall upregulation of *csgD* under ZnO exposure. Significantly upregulated in sample 12 (fold change ~14.73), which indicates stress-induced *csgD* overexpression, possibly due to oxidative stress response or sub-lethal nanoparticle effects. ZnO NPs are known to environmental resistance [39;40]. Both ZnO and Fe_2O_3 NPs induce the upregulation of the *csgD* gene in *E. coli*, likely due to oxidative or metal ion stress, triggering biofilm-related gene expression. ZnO shows greater variability, while Fe_2O_3 elicits a more consistent response. The upregulation of *csgD* biofilm formation may be part of *E. coli*'s adaptive response to nanoparticle-induced stress [41;42]. The increase and general occurrence of multidrug-resistant (MDR) bacteria have become a global public health concern, and *E. coli* is becoming increasingly resistant to many antibiotics, limiting the therapeutic management of infections [43;44]. In addition, metal oxide nanomaterials have revealed greater antibacterial

activity against MDR microbes [45;46].

These findings highlight the critical regulatory role of *CsgD* gene expression in *E. coli* pathogenicity and biofilm formation. Additionally, ZnO NPs have become promising antibacterial agents capable of inhibiting virulence gene expression and biofilm production, particularly in MTD for *E. coli* strains. Disrupting the *CsgD* regulatory pathway could therefore be a strategic target for new anti-biofilm and anti-virulence, especially against UTIs and other disorders associated with biofilm presence. Nonetheless, further in vivo investigations are needed to confirm these in vitro results, verify the safety of ZnO NPs, and determine optimal therapeutic doses for clinical application. The findings suggest promoting ZnO-based antimicrobial formulations as next-generation options to replace conventional antibiotics in treating antibiotic-resistant *E. coli.*

This study indicated that both ZnO and Fe_2O_3 NPs induce upregulation of the *csgD* gene in *E. coli*, suggesting activation of biofilm-related stress responses, and ZnO NPs demonstrated variable but stronger induction, potentially due to ROS generation and membrane stress. Fe_2O_3 NPs elicited a more modest, although present, response, possibly linked to iron-associated stress. These findings highlight the regulatory role of *csgD* in biofilm development under NPs exposure. The ZnO NPs could be promising antibacterial agents targeting biofilm-associated infections. Further in vivo validation is needed to translate these findings into therapeutic applications.

4. Conclusions

This study demonstrated that the transcriptional regulator *csgD* gene expression plays a vital role in controlling key physiological processes in *E. coli*, including biofilm formation, motility, environmental stress responses, and the ability to adapt and survive under stress. The result of ZnO produces upregulation in expression levels for the *csgD* gene compared to Fe_2O_3. The ZnO NPs showed a stronger and more persistent effect in suppressing virulence-associated pathways, particularly under sub-inhibitory doses.

Ethics approval

The local ethical committee at the University of Baghdad approved the project. No animal studies are present in the manuscript and no potentially identified images or data are present in the manuscript.

Funding

This research received no external funding.

Conflicts of interest

The authors declare that they have no competing interests.

Acknowledgments

The authors would like to thank the Department of Biotechnology, College of Science, University of Baghdad, for the support provided during the research. The Iraqi Ministry of Higher Education and Scientific Research also supported this work.

References

[1] H.M. Abbas, M.F. Al Marjani, R. Gdoura, Evaluation of the antibacterial activity of CuO and ZnO nanoparticles against uropathogenic *Escherichia coli*, *J. Taibah Univ. Sci.* 18 (2024) 2322776. https://doi.org/10.1080/16583655.2024.2322776.

[2]A. Markowicz, S. Borymski, A. Adamek, S. Sułowicz, The influence of ZnO nanoparticles on horizontal transfer of resistance genes in lab and soil conditions, *Environ. Res.* 223 (2023) 115420. https://doi.org/10.1016/j.envres.2023.115420.

[3] K.S.P. Cabuhat, L.S. Moron-Espiritu, Quorum sensing orchestrates antibiotic drug resistance, biofilm formation, and motility in *Escherichia coli* and quorum quenching activities of plant-derived natural products: a review, *J. Pure Appl. Microbiol.* 16 (2022) 1538–1549. https://doi.org/10.22207/JPAM.16.3.52.

[4] R.M. Sherif, D. Talat, B.A. Alaidaroos, R.M. Farsi, S.A. Hassoubah, F.A. Jaber, T.M. Azer, R.M. El-Masry, M.E. Abd El-Hack, M.S. Ibrahim, A. Elbestawy, Antimicrobial impacts of zinc oxide nanoparticles on Shiga toxin-producing

Escherichia coli (serotype O26), *Ann. Anim. Sci.* 23 (2023) 461–471. https://doi.org/10.2478/aoas-2022-0088.

[5] F. Zhao, H. Yang, D. Bi, A. Khaledi, M. Qiao, A systematic review and meta-analysis of antibiotic resistance patterns, and the correlation between biofilm formation with virulence factors in uropathogenic *E. coli* isolated from urinary tract infections, *Microb. Pathog.* 144 (2020) 104196. https://doi.org/10.1016/j.micpath.2020.104196.

[6] F.A. El-Shenawy, E.M.E. El-Sherbeny, S. Kassem, Efficacy of zinc oxide and copper oxide nanoparticles on virulence genes of avian pathogenic *E. coli* (APEC) in broilers, *BMC Vet. Res.* 19 (2023) 108. https://doi.org/10.1186/s12917-023-3643.

[7] B. Gunes, A critical review on biofilm-based reactor systems for enhanced syngas fermentation processes, *Renew. Sustain. Energy Rev.* 143 (2021) 110950. https://doi.org/10.1016/j.rser.2021.110950.

[8] A.O. Fadwa, A.M. Albarag, D.K. Alkoblan, A. Mateen, Determination of synergistic effects of antibiotics and ZnO NPs against isolated *E. coli* and *A. baumannii* bacterial strains from clinical samples, *Saudi J. Biol. Sci.* 28 (2021) 5332–5337. https://doi.org/10.1016/j.sjbs.2021.05.057.

[9] C. Monteiro, I. Saxena, X. Wang, A. Kader, R. Offer, Biofilm-relevant genes in *Escherichia coli* and their control by intra- and extracellular signals (Doctoral dissertation, Lebenswissenschaftliche Fakultät), 2025. https://doi.org/10.18452/32758.

[10] C.H. Yan, F.H. Chen, Y.L. Yang, Y.F. Zhan, R.A. Herman, L.C. Gong, S. Sheng, J. Wang, The transcription factor CsgD contributes to engineered *Escherichia coli* resistance by regulating biofilm formation and stress responses, *Int. J. Mol. Sci.* 24 (2023) 13681. https://doi.org/10.3390/ijms241813681.

[11] J.D. García-García, L.M. Contreras-Alvarado, A. Cruz-Córdova, R. Hernández-Castro, M. Flores-Encarnacion, S. Rivera-Gutiérrez, J. Arellano-Galindo, S.A. Ochoa, J. Xicohtencatl-Cortes, Pathogenesis and immunomodulation of urinary tract infections caused by uropathogenic *Escherichia coli*, *Microorganisms* 13 (2025) 745. https://doi.org/10.3390/microorganisms13040745.

[12] S.A. Bustin, V. Benes, J.A. Garson, J. Hellemans, J. Huggett, M. Kubista, R. Mueller, T. Nolan, M.W. Pfaffl, G.L. Shipley, J. Vandesompele, The MIQE guidelines: Minimum information for publication of quantitative real-time PCR experiments, *Clin. Chem.* 55 (2009) 611–622. https://doi.org/10.1373/clinchem.2008.112797.

[13] M.W.W. Azam, A.U.U. Khan, CRISPRi-mediated suppression of *E. coli* Nissle 1917 virulence factors: A strategy for creating an engineered probiotic using *csgD* gene suppression, *Front. Nutr.* 9 (2022) 938989. https://doi.org/10.3389/fnut.2022.938989.

[14] J. Zhang, T. Feng, J. Wang, Y. Wang, X.H. Zhang, The mechanisms and applications of quorum sensing (QS) and quorum quenching (QQ), *J. Ocean Univ. China* 18 (2019) 1427–1442. https://doi.org/10.1016/j.micpath.2020.104196.

[15] A.M. Sheiha, S.A. Abdelnour, M.E. Abd El-Hack, A.F. Khafaga, K.A. Metwally, J.S. Ajarem, M.T. El-Saadony, Effects of dietary biological or chemical-synthesized nano-selenium supplementation on growing rabbits exposed to thermal stress, *Animals* 10 (2020) 430. https://doi.org/10.3390/ani10030430.

[16] M. Alagawany, S.Y. Qattan, Y.A. Attia, M.T. El-Saadony, S.S. Elnesr, M.A. Mahmoud, M.E. Abd El-Hack, F.M. Reda, Use of chemical nano-selenium as an antibacterial and antifungal agent in quail diets and its effect on growth, carcasses, antioxidant, immunity, and caecal microbes, *Animals* 11 (2021) 3027. https://doi.org/10.3390/ani11113027.

[17] S.E. Murinda, A.M. Ibekwe, N.G. Rodriguez, K.L. Quiroz, A.P. Mujica, K. Osmon, Shiga toxin–producing *Escherichia coli* in mastitis: An international perspective, *Foodborne Pathog. Dis.* 16 (2019) 4. https://doi.org/10.1089/fpd.2018.2491.

[18] M. Alshammari, A. Ahmad, M. AlKhulaifi, D. Al Farraj, S. Alsudir, M. Alarawi, G. Takashi, E. Alyamani, Reduction of biofilm formation of *Escherichia coli* by targeting quorum sensing and adhesion genes using the CRISPR/Cas9-HDR approach, and its clinical application on urinary catheter, *J. Infect. Public Health* 16

(2023) 1174–1183. https://doi.org/10.1016/j.jiph.2023.05.026.

[19] D. Buchmann, M. Schwabe, R. Weiss, A.W. Kuss, K. Schaufler, R. Schlüter, S. Rödiger, S. Guenther, N. Schultze, Natural phenolic compounds as biofilm inhibitors of multidrug-resistant *Escherichia coli* – the role of similar biological processes despite structural diversity, *Front. Microbiol.* 14 (2023) 1232039. https://doi.org/10.3389/fmicb.2023.1232039.

[20] M.E. Abd El-Hack, M.T. El-Saadony, A.M. Saad, H.M. Salem, N.M. Ashry, M.M.A. Ghanima, K.A. El-Tarabily, Essential oils and their nanoemulsions as green alternatives to antibiotics in poultry nutrition: A comprehensive review, *Poult. Sci.* 101 (2021) 101584. https://doi.org/10.1016/j.psj.2021.101584.

[21] N.A. Al-Gabri, S.A. Saghir, S.A. Al-Hashedi, A.H. El-Far, A.F. Khafaga, A.A. Swelum, K.A. El-Tarabily, Therapeutic potential of thymoquinone and its nanoformulations in pulmonary injury: a comprehensive review, *Int. J. Nanomed.* 16 (2021) 2735–2758. https://doi.org/10.2147/IJN.S314321.

[22] B. Asgari, J.R. Burke, B.L. Quigley, G. Bradford, E. Hatje, A. Kuballa, M. Katouli, Identification of virulence genes associated with pathogenicity of translocating *Escherichia coli* with special reference to the type 6 secretion system, *Microorganisms* 12 (2024) 1851. https://doi.org/10.3390/microorganisms12091851.

[23] A.A.M. Al Mamun, K. Kissoon, Y.G. Li, E. Hancock, P.J. Christie, The F plasmid conjutome: the repertoire of *E. coli* proteins translocated through an F-encoded type IV secretion system, *mSphere* 9 (2024) e00354-24. https://doi.org/10.1128/msphere.00354-24.

[24] F. Islam, S. Shohag, M.J. Uddin, M.R. Islam, M.H. Nafady, A. Akter, S. Mitra, A. Roy, T.B. Emran, S. Cavalu, Exploring the journey of zinc oxide nanoparticles (ZnO-NPs) toward biomedical applications, *Materials* 15 (2022) 2160. https://doi.org/10.3390/ma15062160.

[25] N. Yehia, M.A. AbdelSabour, A.M. Erfan, Z.M. Ali, R.A. Soliman, A. Samy, M.E. Abd El-Hack, K.A. Ahmed, Selenium nanoparticles enhance the efficacy of homologous vaccine against the highly pathogenic avian influenza H5N1 virus in chickens, *Saudi J. Biol. Sci.* 29 (2022) 2095–2111. https://doi.org/10.1016/j.sjbs.2021.11.051.

[26] H.K. Al-Qazzaz, Impact of DNA methylation and gene expression of *H19*, *SNRPN* and *LINE-1* genes on oligospermic men infertility (Doctoral dissertation, University of Baghdad), 2021.

[27] D. Stepanov, D. Buchmann, N. Schultze, G. Wolber, K. Schaufler, S. Guenther, et al., A combined Bayesian and similarity-based approach for predicting *E. coli* biofilm inhibition by phenolic natural compounds, *J. Nat. Prod.* 85 (2022) 2255–2265. https://doi.org/10.1021/acs.jnatprod.2c00005.

[28] S.A. Hussen, S.M. Abed, H.S. Ahmad, Detection of biofilm forming bacteria causing otitis media infection, *Samarra J. Pure Appl. Sci.* 6 (2024) 110–127. https://doi.org/10.54153/sjpas.2024.v6i2/2.672.

[29] M. Balouiri, M. Sadiki, S.K. Ibnsouda, Methods for *in vitro* evaluating antimicrobial activity: a review, *J. Pharm. Anal.* 6 (2016) 71–79. https://doi.org/10.1016/j.jpha.2015.11.005.

[30] G. Tortella Fuentes, P. Fincheira, O. Rubilar, S. Leiva, I. Fernandez, M. Schoebitz, M.T. Pelegrino, A. Paganotti, R.A. Dos Reis, A.B. Seabra, Nanoparticle-based nitric oxide donors: exploring their antimicrobial and anti-biofilm capabilities, *Antibiotics* 13 (2024) 1047. https://doi.org/10.3390/antibiotics13111047.

[31] A.L. Flores-Mireles, J.N. Walker, M. Caparon, S.J. Hultgren, Urinary tract infections: epidemiology, mechanisms of infection and treatment options, *Nat. Rev. Microbiol.* 13 (2015) 269–284. https://doi.org/10.1038/nrmicro3432.

[32] S. Ghosh, M. Nag, D. Lahiri, T. Sarkar, S. Pati, Z.A. Kari, N.P. Nirmal, H.A. Edinur, R.R. Ray, Engineered biofilm: innovative nextgen strategy for quality enhancement of fermented foods, *Front. Nutr.* 9 (2022) 808630. https://doi.org/10.3389/fnut.2022.808630.

[33] T. George, V. Sivam, M. Vaiyapuri, R. Anandan,

G.K. Sivaraman, T.C. Joseph, Standardizing biofilm quantification: harmonizing crystal violet absorbance measurements through extinction coefficient ratio adjustment, *Arch. Microbiol.* 207 (2025) 1–7. https://doi.org/10.1007/s00203-025-04251-0.

[34] M.M. Khalaf, M. Gouda, M.F. Abou Taleb, F.E. Al-Rasheed, H.M. Abd El-Lateef, Bioinspired synthesis of Fe_2O_3 nanoparticles using *Rosa rugosa* flower extract and their application as a potent alternative disinfecting agent against waterborne pathogens within wastewater management, *J. Taiwan Inst. Chem. Eng.* 171 (2025) 106079. https://doi.org/10.1016/j.jtice.2025.106079 .

[35] Q. Bonet-Rossinyol, C. Camprubí-Font, M. López-Siles, M. Martinez-Medina, Identification of differences in gene expression implicated in the adherent-invasive *Escherichia coli* phenotype during *in vitro* infection of intestinal epithelial cells, *Front. Cell. Infect. Microbiol.* 13 (2023) 1228159. https://doi.org/10.3389/fcimb.2023.1228159.

[36] A. Zuberi, M.W. Azam, A.U. Khan, CRISPR interference (CRISPRi)-mediated suppression of *ompR* gene in *E. coli*: an alternative approach to inhibit biofilm, *Curr. Microbiol.* 79 (2022) 1–10. https://doi.org/10.1007/s00284-021-02760-x.

[37] S. Nadar, T. Khan, S.G. Patching, A. Omri, Development of antibiofilm therapeutics strategies to overcome antimicrobial drug resistance, *Microorganisms* 10 (2022) 303. https://doi.org/10.3390/microorganisms10020303.

[38] Y.K. Mohanta, I. Chakrabartty, A.K. Mishra, H. Chopra, S. Mahanta, S.K. Avula, K. Patowary, R. Ahmed, B. Mishra, T.K. Mohanta, M. Saravanan, Nanotechnology in combating biofilm: a smart and promising therapeutic strategy, *Front. Microbiol.* 13 (2023) 1028086. https://doi.org/10.3389/fmicb.2022.1028086.

[39] A. Laith, Y. Yaaqoob, The effect of zinc oxide and silver nanoparticles on *rsmA* and *rsbA* expression in *Proteus mirabilis*, *Int. J. Pharm. Biomed. Sci.* 3 (2023) 6. https://doi.org/10.47191/ijpbms/v3-i6-07.

[40] J.A. Salman, A.A. Kadhim, G.A. Ismail, Effect of biosynthesized zinc oxide nanoparticles against MDR pathogenic bacteria isolated from wounds and burns, *Iraqi J. Biotechnol.* 24 (2025) SI.

[41] H. Chen, C.H. Yan, Y.F. Zhan, L.T. Geng, L.L. Zhu, L.C. Gong, J. Wang, Boron derivatives accelerate biofilm formation of recombinant *Escherichia coli* via increasing quorum sensing system autoinducer-2 activity, *Int. J. Mol. Sci.* 23 (2022) 8059. https://doi.org/10.3390/ijms23158059.

[42] O. Al Rugaie, M.R. Abdulbaqi, A.W. Danial, H.A. Mohammed, M. Alsharidah, H.M. Tawfeek, A.A. Abdellatif, Potential application of *Origanum majorana* stabilized silver nanoparticles for coating of urinary catheter, *Drug Des. Devel. Ther.* 31 (2025) 2941–2957. https://doi.org/10.2147/DDDT.S512320.

[43] P. Dawadi, S. Khanal, T. Prasai Joshi, S. Kc, R. Tuladhar, B.L. Maharjan, A. Darai, D.R. Joshi, Antibiotic resistance, biofilm formation and sub-inhibitory hydrogen peroxide stimulation in uropathogenic *Escherichia coli*, *Microbiol. Insights* (2022) 11786361221135224. https://doi.org/10.1177/11786361221135224.

[44] M.T. Elabbasy, R.M. El Bayomi, E.A. Abdelkarim, A.E. Hafez, M.S. Othman, M.E. Ghoniem, M.A. Samak, M.H. Alshammari, F.A. Almarshadi, T. Elsamahy, M.A. Hussein, Antibacterial and antibiofilm activity of green-synthesized zinc oxide nanoparticles against multidrug-resistant *Escherichia coli* isolated from retail fish, *Molecules* 30 (2025) 768. https://doi.org/10.3390/molecules30040768.

[45] M. Idrees, S. Sawant, N. Karodia, A. Rahman, *Staphylococcus aureus* biofilm: morphology, genetics, pathogenesis, and treatment strategies, *Int. J. Environ. Res. Public Health* 18 (2021) 7602. https://doi.org/10.3390/ijerph18147602.

[46] R.I. Muntaha, The effectiveness of *Salvadora persica* extracted miswak and ZnO NPs on pathogenic bacteria, *Int. J. Drug Deliv. Technol.* 13 (2023) 224–236. https://doi.org/10.25258/ijddt.13.1.37.